Vibronic treatment of vibrational excitation and electron capture in $H^+ + H_2$ (HD, D_2, ...) collisions at low impact energies

L. F. Errea, L. Fernández,* L. Méndez, B. Pons,† I. Rabadán, and A. Riera
Laboratorio Asociado al CIEMAT de Física Atómica y Molecular en Plasmas de Fusión, Departamento de Química, Universidad Autónoma de Madrid, Madrid-28049, Spain
(Received 21 December 2006; published 6 March 2007)

We present *ab initio* calculations of cross sections for vibrational excitation and electron capture in collisions of H^+ with H_2 and its isotopical variants at impact energies between 10 eV and 10 keV. Calculations have been carried out by means of a vibronic close-coupling expansion in both quantal and semiclassical treatments to evaluate vibrationally resolved total cross sections. We also report total cross sections and spectra for dissociative capture and H_2 dissociation.

DOI: 10.1103/PhysRevA.75.032703 PACS number(s): 34.70.+e, 34.50.−s

I. INTRODUCTION

The collision of H^+ with H_2 is a benchmark system of ion-molecule collisions, and it is also important in fusion plasmas (e.g., [1]) and in the interaction of the solar wind with cometary and planetary atmospheres (e.g. [2]). In this work, we consider theoretically this collision at impact energies between 10 eV and 10 keV, where cross sections for ionization are small [3–5] and the most significant processes are the following:

(i) Vibrational excitation:

$$H^+ + H_2(X\,^1\Sigma_g^+, \nu = 0) \rightarrow H^+ + H_2(X\,^1\Sigma_g^+, \nu'). \quad (1)$$

(ii) Dissociation:

$$H^+ + H_2(X\,^1\Sigma_g^+, \nu = 0) \rightarrow H^+ + H(1s) + H(1s). \quad (2)$$

(iii) Electron capture:

$$H^+ + H_2(X\,^1\Sigma_g^+, \nu = 0) \rightarrow H(1s) + H_2^+(X\,^1\Sigma_g^+, \nu'). \quad (3)$$

(iv) Dissociative capture:

$$H^+ + H_2(X\,^1\Sigma_g^+, \nu = 0) \rightarrow H(1s) + H^+ + H(1s). \quad (4)$$

Given its fundamental character, many works have considered $H^+ + H_2$ collisions. A review of them (before 1990) can be found in [6] and fittings of the tabulated data in [7]. In the energy range of the present calculation, total cross sections for electron capture have been measured in Ref. [8] and the electron-capture cross sections from different isotopic species have been reported in [9,10], but measurements of vibrational excitation and dissociative capture are not available. From the theoretical side, Baer *et al.* [11] carried out calculations at $E=30$ eV, using the infinite-order sudden-approximation (IOSA) method. The IOSA method was also applied by Krstić [12] and Krstić and Janev [13] for $E<15$ eV; these authors evaluated dissociative capture and excitation cross sections by including in the expansion a discretized representation of H_2 and H_2^+ vibrational continua. $H^+ + H_2$ collisions have also been addressed by Morales *et al.* [14], using the electron-nuclear dynamics (END) method, in which the nuclear motion is described classically, and by Niedner *et al.* [15] and Ichihara *et al.* [16], applying the trajectory-surface-hopping (TSH) method [17].

Previous calculations at high energy ($E>50$ eV) employed an eikonal semiclassical treatment, where the projectile follows a rectilinear trajectory. At these energies, target vibration and rotation are described by means of the sudden approximation, or the simpler Franck-Condon (FC) approximation. In the sudden approximation eikonal method (called the SEIKON approximation in [18]), one assumes that the initial rovibrational wave function does not change while electronic transitions take place; in the FC approximation, the target H-H internuclear distance does not change during the collision. In particular, the early calculation of Kimura [19] used the FC approximation to evaluate the nonadiabatic couplings between vibronic adiabatic wave functions. Elizaga *et al.* [20] applied FC and SEIKON approximations and showed that the latter approach yields better agreement with the experimental cross sections for electron capture. However, at $E<200$ eV, the cross section calculated in [20] (and also those reported in Refs. [9,10], obtained with the method of [19]) rapidly decreases, showing a poor agreement with the experiment. This behavior was explained in [21] as a consequence of the mechanism of the capture process. At high energies, a sudden mechanism takes place where the electronic transition is so fast that the H_2 initial vibrational wave function remains unchanged, and the vibrational states of H_2^+ are populated, after the electronic transition, by projection of the initial vibrational wave function on the exit channels; the relative populations of these vibrational states are then roughly given by the values of the FC factors between $H_2(X\,^1\Sigma_g^+, \nu=0)$ and $H_2^+(X\,^2\Sigma_g^+, \nu')$ wave functions, yielding a maximum population for $\nu' \simeq 3$. As E decreases, a quasiresonant two-step mechanism [15] becomes dominant; the first step is the vibrational excitation of H_2 and the second one involves transitions from these vibrational excited states to quasidegenerate capture states. In particular, the energies of $H_2(X\,^1\Sigma_g^+, \nu=4)$ and $H_2^+(X\,^2\Sigma_g^+, \nu'=0)$ are very close, and now $\nu'=0$ is the most populated vibrational level.

*Present address: Institut für Theoretische Physik. TU-Clausthal. Leibnizstraße 10. D-38678 Clausthal-Zellerfeld, Germany.

†Centre de Lasers Intenses et Applications. Université de Bordeaux-I-CNRS-CEA. 351 Cours de la Liberation 33405, Talence, France.

In practice, the SEIKON approximation cannot describe the quasiresonant mechanism, and a treatment beyond this approximation is therefore required. It must be pointed out that the two-step mechanism is deduced in [21] *a posteriori* from the analysis of the transition probabilities, but it is not introduced *ad hoc* as erroneously interpreted in [10].

The aim of the present work is to apply a vibronic close-coupling (VCC) formalism to carry out calculations in an extended energy range (0.01–10 keV). Our treatment is based on that of [21], which has been improved in three aspects: (a) We have improved the vibrational basis set in order to describe dissociative processes. (b) We have employed a larger space of nuclear configurations, including regions near the asymptotic conical seam, which have required the use of a diabatic basis set to regularize the nonadiabatic couplings. (c) We have applied quantal and semiclassical treatments for the projectile-target relative motions. More specifically, with respect to the first point, previous works of our group for multicharged-ion–H_2 collisions [18,22] pointed out that capture into H_2^+ vibrational continuum states could be competitive with nondissociative capture at $E<100$ eV, and therefore, this could limit the accuracy of the expansion of [21] that did not include continuum states. In the present work we have employed a basis set of spherical Bessel functions, which is more appropriate than the Gaussian basis set of [21] to accurately describe the vibrational continuum. With respect to the second point, the calculation of total capture cross sections applying treatments based on the sudden approximation only requires one to consider internuclear distances of the target molecule, ρ, near the H_2 equilibrium distance $\rho_0 \simeq 1.4$ a.u., which does not significantly change during the nonadiabatic transitions. However, in VCC calculations a larger range of ρ values is needed, in particular to study dissociative processes, and, besides the additional computational effort required, an important difficulty for the $H^+ + H_2$ system is the presence of a conical seam between the two lowest potential energy surfaces of H_3^+; it appears at $\rho \simeq 2.45$ a.u. and for $R \to \infty$, where R is the distance between the projectile nucleus and the nuclear center of mass of the diatomic molecule. Since the dynamical couplings are singular in the conical intersections, we have applied a regularization procedure (see [23] and references therein) to avoid this difficulty. With respect to the third point, calculations with nuclear straight-line trajectories of Ref. [21] may be inaccurate at $E<50$ eV. Accordingly, we have used a full quantum mechanical treatment to compare with previous calculations at $E=30$ eV. This comparison is also interesting given that previous calculations employed DIM semiempirical wave functions [24] while we use *ab initio* ones.

The paper is organized as follows: The details of dynamical methods and molecular calculation are presented in Sec. II, the method for regularizing the couplings in the neighborhood of the conical intersection is described in Sec. III, our results are shown in Sec. IV, and the main conclusions are outlined in Sec. V. Atomic units are used unless otherwise stated.

II. METHOD

A. Quantal formalism

At low energies we have applied a quantal treatment within the IOSA treatment (see, e.g., [25]), which employs the sudden approximation for molecular rotation. At the collision energies considered in this work, the rotation periods of the diatomic molecules H_2 and H_2^+ are large compared to the collision characteristic time, and one can assume that the rotational state does not change during the collision. Accordingly, to simplify the notation, we have omitted in the following equations the rotational component of the collision wave function Ψ; this wave function is expanded in a vibronic basis set $\{\psi_i\, \chi_{i\nu}\}$:

$$\Psi(\boldsymbol{r},\boldsymbol{\rho};\boldsymbol{\xi}) = \sum_l \sum_{i\nu} F^l_{i\nu}(\xi) Y_{lm}(\hat{\xi}) \psi_i(\boldsymbol{r},\boldsymbol{\rho};\boldsymbol{\xi}) \chi_{i\nu}(\rho), \qquad (5)$$

where $\boldsymbol{r}$ denotes the set of electronic coordinates referred to the nuclear center of mass, $\boldsymbol{\rho}$ the vector that joins the two nuclei of the target molecule, and $\boldsymbol{\xi}(\boldsymbol{r},\boldsymbol{R})$ is a common reaction coordinate (CRC) [26], which is introduced to ensure that the expansion (5) fulfills the collision boundary conditions. It has the form

$$\boldsymbol{\xi}(\boldsymbol{r},\boldsymbol{R}) = \boldsymbol{R} + \frac{1}{M}\sum_{i=1}^{N}\left[f(\boldsymbol{r}_i,R)\boldsymbol{r}_i - \frac{1}{2}f^2(\boldsymbol{r}_i,R)\boldsymbol{R}\right], \qquad (6)$$

where N is the number of electrons and $f(\boldsymbol{r}_i,R)$ is a switching function (in the present calculation we have employed the function proposed in [27]). $Y_{lm}(\hat{\xi})$ are spherical harmonics and $F^l_{i\nu}$ are the nuclear functions, which are obtained by solving the Schrödinger equation

$$\left[-\frac{1}{2M}\nabla_R^2 + \mathrm{H}_{\mathrm{elec}} + T_{\mathrm{vib}} - E\right]\Psi(\boldsymbol{r},\boldsymbol{\rho};\boldsymbol{\xi}) = 0, \qquad (7)$$

with M the reduced mass of the ion with respect to the molecular target and E the impact energy in the center-of-mass reference frame. The functions $\psi_i(\boldsymbol{r},\boldsymbol{\rho};\boldsymbol{\xi})$ are eigenfunctions of electronic Born-Oppenheimer Hamiltonian for fixed nuclei,

$$\mathrm{H}_{\mathrm{elec}}\psi_i(\boldsymbol{r};\boldsymbol{\rho},\boldsymbol{R}) = E_i(\boldsymbol{\rho},\boldsymbol{R})\psi_i(\boldsymbol{r};\boldsymbol{\rho},\boldsymbol{R}), \qquad (8)$$

and $\chi_{i\nu}(\rho)$ are eigenfunctions of the vibrational Hamiltonian operators for the diatomic molecules,

$$[T_{\mathrm{vib}} + E_i^{\infty}(\rho)]\chi_{i\nu}(\rho) = E_{i\nu}\chi_{i\nu}(\rho), \qquad (9)$$

where the potentials E_i^{∞} are the asymptotic values of the electronic energies E_i at infinite separation between the projectile and target. Substitution of expansion (5) into Eq. (7) leads to a set of differential equations for the nuclear functions $F^l_{i\nu}$. In particular, in the IOSA method, the Coriolis couplings are neglected and partial waves with different values of l are uncoupled, which yields the system of differential equations

$$\frac{1}{2M}\left[-\frac{d^2}{d\xi^2} + \frac{l(l+1)}{\xi^2} - k_{i\nu}^2\right]F^l_{i\nu} = \sum_{i'\nu'}\Omega_{ii'\nu\nu'}F^l_{i'\nu'}, \qquad (10)$$

with

$$k_{i\nu}^2 = 2M(E - E_{i\nu} - \epsilon_{i\nu}) \tag{11}$$

and

$$\epsilon_{i\nu}(\xi,\theta) = \langle \chi_{i\nu}|E_i(\rho,\xi,\theta) - E_i^{\infty}(\rho)|\chi_{i\nu}\rangle_\rho. \tag{12}$$

In the IOSA, the couplings $\Omega_{i\nu i'\nu'}$ depend parametrically on the angle θ between $\mathbf{R}$ and $\boldsymbol{\rho}$. They are given by

$$\Omega_{i\nu j\mu}(R,\theta) = -\frac{1}{2M}\left[\langle \chi_{i\nu}|\mathcal{R}_{ij}|\chi_{j\mu}\rangle + \left\langle \psi_i \left| \frac{\partial^2}{\partial \xi^2} \right| \psi_j \right\rangle\right] + \tilde{H}_{i\nu i\mu}\delta_{ij} - \frac{1}{2m}\mathcal{P}_{i\nu j\mu}, \tag{13}$$

where

$$\mathcal{R}_{ij} = 2\left[\left\langle \psi_i \left| \frac{\partial}{\partial \xi} \right| \psi_j \right\rangle + A_{ij}^R\right]\frac{d}{d\xi},$$

$$\mathcal{P}_{i\nu j\mu} = \left\langle \left\langle \psi_i \left| \frac{\partial}{\partial \rho} \right| \psi_j \right\rangle_{\mathbf{r}} \left(\chi_{i\nu}\frac{\partial \chi_{j\mu}}{\partial \rho} - \chi_{j\mu}\frac{\partial \chi_{i\nu}}{\partial \rho}\right)\right\rangle_\rho,$$

$$\tilde{H}_{i\nu i\mu} = \langle \chi_{i\nu}|E_i(\rho,\xi) - E_i^{\infty}(\rho)|\chi_{i\mu}\rangle, \tag{14}$$

and where m is the nuclear reduced mass of the molecule. A_{ij}^R are the correction terms introduced by the CRC that ensure that the couplings vanish asymptotically. In the present calculation we have kept these terms up to first order in $1/M$, as explained in [28].

In practice, a unitary transformation is carried out to obtain diabatic vibronic states for which the radial couplings $\mathcal{R}_{ij}$ vanish. Using closure [29], the matrix elements of $(\partial^2/\partial\xi^2)$ in a diabatic basis are expected to be very small and neglected, and the couplings in this basis become

$$\Omega_{i\nu j\mu}^d = -\langle \psi_i^d \chi_{i\nu}|H_{\text{elec}}|\psi_j^d \chi_{j\mu}\rangle + \tilde{H}_{i\nu j\mu}^d\delta_{ij} - \frac{1}{2m}\mathcal{P}_{i\nu j\mu}^d. \tag{15}$$

Use of standard collision theory (see, e.g., [30] and references therein) allows one to obtain the scattering matrix elements $S_{i\nu j\mu}^l$ from the solutions of Eq. (10), which lead to the total cross sections. In particular, the total cross section for transition from the initial state $\psi_I\chi_{IY}$ to the final state $\psi_F\chi_{F\Phi}$, $\sigma_{IYF\Phi}$, is given by

$$\sigma_{IYF\Phi} = \frac{\pi}{k_I^2}\sum_l (2l+1)|S_{IYF\Phi}^l|^2, \tag{16}$$

where k_I is the initial momentum. Since the couplings depend on θ, the cross sections of Eq. (16) are functions of this parameter and the orientation-averaged cross sections read

$$\bar{\sigma}_{IYF\Phi} = \int_0^{\pi/2} d\theta \sin\theta \sigma_{IYF\Phi}. \tag{17}$$

B. Semiclassical formalism

At high energies, we have applied the semiclassical eikonal approximation where the projectile-target relative motion is treated classically by means of a rectilinear trajectory $\mathbf{R} = \mathbf{b} + \mathbf{v}t$. The collision wave function Ψ^{SC} is now a solution of

$$\left[H_{\text{elec}} + T_{\text{vib}} - i\left.\frac{\partial}{\partial t}\right|_{\mathbf{r}}\right]\Psi^{SC} = 0. \tag{18}$$

As in the quantal case, we have applied the sudden approximation for rotation and expanded the function Ψ^{SC} in the vibronic basis set $\{\psi_i\chi_{i\nu}\}$:

$$\Psi^{SC}(\boldsymbol{r},\boldsymbol{\rho},t) = D(\boldsymbol{r},\boldsymbol{R})\sum_{i\nu} a_{i\nu}(t)\psi_i(\boldsymbol{r},\boldsymbol{\rho};\boldsymbol{R})\chi_{i\nu}(\rho) \times \exp\left(-i\left[\int_0^t dt'\,\epsilon_{i\nu}(t') + E_{i\nu}t\right]\right), \tag{19}$$

where D is a common translation factor (CTF) [31], defined in terms of the same switching function as the CRC (6). Substitution of expansion (19) in the eikonal equation (18) leads to the set of differential equations

$$i\frac{da_{i\nu}}{dt} = \sum_{j\mu}\left\langle D\psi_i\chi_{i\nu}\left|H_{\text{elec}} + T_{\text{vib}} - i\frac{\partial}{\partial t}\right|D\psi_j\chi_{j\mu}\right\rangle_{r\rho} a_{j\mu} \times \exp\left(i\int_0^t (\epsilon_{i\nu} + E_{i\nu} - \epsilon_{j\mu} - E_{j\mu})dt'\right), \tag{20}$$

whose solutions are the coefficients $a_{i\nu}$. The dynamical couplings are

$$\left\langle D\psi_i\chi_{i\nu}\left|H_{\text{elec}} + T_{\text{vib}} - i\frac{\partial}{\partial t}\right|D\psi_j\chi_{j\mu}\right\rangle_{r\rho} = \langle \chi_{i\nu}|\mathcal{A}_{ij}|\chi_{j\mu}\rangle_\rho + \tilde{H}_{i\nu j\mu}\delta_{ij} - \frac{1}{2m}\mathcal{P}_{i\nu j\mu}, \tag{21}$$

where $\tilde{H}_{i\nu i\mu}$ and $P_{i\nu j\mu}$ are defined in (14). As the CRC and the CTF employ the same switching function, the couplings $\mathcal{A}_{ij} = \langle D\psi_i|H_{\text{elec}} - i\frac{\partial}{\partial t}|D\psi_j\rangle_{\mathbf{r}}$ are identical to the corresponding ones in the quantal formalism [28], although in the IOSA method only the radial components $\mathcal{R}_{ij}$ of $\mathcal{A}_{ij}$ are kept.

The total cross section $\sigma_{IYF\Phi}$ is given in the semiclassical formalism by

$$\sigma_{IYF\Phi} = 2\pi\int_0^\infty b\,db\,P_{IYF\Phi}(b), \tag{22}$$

where the transition probability $P_{IYF\Phi}(b)$ is

$$P_{IYF\Phi}(b) = \lim_{t\to\infty}|a_{F\Phi}(t;b)|^2. \tag{23}$$

C. Molecular calculations

The electronic wave functions and potential energy surfaces (PES's) are obtained using a self-consistent-field configuration-interaction method by means of the program MELD [32] and employing a basis set of Gaussian-type orbitals. In a first step, a restricted Hartree-Fock calculation is performed to obtain the molecular orbitals (MO's) of the H_3^+ quasimolecule. A full configuration interaction is then carried out.

The dynamical coupling of Eqs. (15) and (21) is expressed in terms of the gradient matrix elements:

$$V_{ij} = \left\langle \psi_i \left| \frac{\partial \psi_j}{\partial \rho} \right|_{\theta,R} \right\rangle_r, \tag{24}$$

$$M_{ij} = \left\langle \psi_i \left| \frac{\partial \psi_j}{\partial R} \right|_{\theta,\rho} \right\rangle_r + A_{ij}^R(\rho,R,\theta), \tag{25}$$

$$R_{ij} = \left\langle \psi_i \left| \frac{\partial \psi_j}{\partial \theta} \right|_{\rho,R} \right\rangle_r + A_{ij}^\theta(\rho,R,\theta), \tag{26}$$

which are called vibrational, radial, and rotational couplings, respectively. In these equations, $A_{ij}^{R,\theta}$ are the corrections due to the CTF or the CRC. The translation factor also introduces terms proportional to v^2, which have been neglected because they are weak in the velocity range ($v<0.63$ a.u.) of the present calculation.

D. Calculation of vibrational functions

We have drawn from previous studies on the requisites of a reliable description of ionization in ion-atom collisions [33–36] to build both bound and unbound vibrational wave functions as follows: The ρ space is reduced to a hermetic spherical box of (large) radius $\rho_{\max}$, beyond which the vibrational wave functions are assumed to vanish. Since only discrete values of the momentum, $p=\sqrt{2mE_{i\nu}}$, allow one to fulfill the condition $\chi_{i\nu}(\rho_{\max})=0$, the vibrational spectrum reduces to an infinite but discrete set of stationary modes, equally spaced in momentum space by $\Delta p=\pi\rho_{\max}^{-1}$. Within the box, the vibrational functions are obtained by diagonalizing the Hamiltonian matrix [see Eq. (9)] in the basis of all spherical Bessel functions $j_0(k_i\rho)$ with $k_i=i\pi/\rho_{\max}$, such that $j_0(k_i\rho_{\max})=0$ and $0\leqslant k_i\leqslant k_{\max}$. In this work, we have checked the convergence of the vibrational basis set (see Sec. IV B). In general we have used a basis set with $\rho_{\max}=10$ a.u. and a maximum momentum $k_{\max}=40$ a.u.

III. REGULARIZATION OF COUPLINGS IN CONICAL INTERSECTIONS

At each value of the angle θ and for large values of R, the two lowest PES's of H_3^+ show an avoided crossing at $\rho\simeq 2.45$ a.u. These avoided crossings become narrower as R increases and tend to conical intersections (CI's) for $R\to\infty$. This behavior is illustrated in Fig. 1. The presence of the conical seam gives rise to singular couplings, as has been illustrated in detail in [37]. In particular, if we consider the couplings as functions of ρ, for constant R, the vibrational coupling V_{12} shows a peak that tends to a δ function in the limit $R\to\infty$, while the radial coupling R_{12} abruptly changes sign, as may be noted in the left panels of Fig. 2, where we have plotted contour plots for these two couplings as functions of R and ρ.

To regularize the couplings we have defined a diabatic basis set $\{\phi_1,\phi_2\}$ through the unitary transformation

$$\psi_1 = \phi_1 \cos\Theta + \phi_2 \sin\Theta,$$

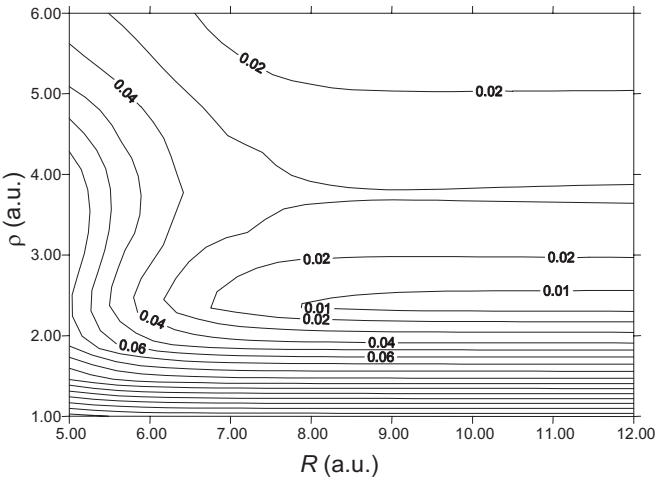

FIG. 1. Contour plot of the difference between the two lowest PES's of H_3^+ for $\theta=60°$. Energy differences smaller than 0.01 a.u. are not shown.

$$\psi_2 = -\phi_1 \sin\Theta + \phi_2 \cos\Theta, \tag{27}$$

where the angle Θ is a function of the nuclear variables ρ and R. The regularized couplings are related to the adiabatic ones by

$$V_{12}^d = V_{12} + \frac{\partial\Theta}{\partial\rho},$$

$$R_{12}^d = R_{12} + \frac{\partial\Theta}{\partial R}, \tag{28}$$

and the nondiagonal Hamiltonian term is

$$H_{12} = -\frac{1}{2}\sin(2\Theta)(E_2 - E_1). \tag{29}$$

As in Refs. [37,38], we have employed a model where the diabatic-energy difference varies linearly with ρ and the nondiagonal Hamiltonian term decays exponentially as a function of R:

$$H_{11} - H_{22} = d(\rho - \rho_0)$$

$$H_{12} = k\, e^{-\beta R}, \tag{30}$$

which leads to

$$\tan(2\Theta) = \frac{2H_{12}}{H_{11}-H_{22}} = \frac{ke^{-\beta R}}{d(\rho-\rho_0)} = \frac{Ae^{-\beta R}}{\rho-\rho_0}, \tag{31}$$

where the parameters ρ_0, A, and β are obtained by nonlinear curve fitting of the adiabatic dynamical couplings in the region $\rho\approx\rho_0$. In order to improve this fitting, we have allowed an exponential variation of ρ_0 (the center of the CI), with R:

$$\rho_0 = \rho_\infty + B\, e^{-\gamma R}, \tag{32}$$

which yields three additional parameters ρ_∞, B, and γ.

In Fig. 2 we compare the couplings V_{12} and R_{12} in diabatic and adiabatic bases [see Eq. (28)], where we show that the singular behavior of those couplings has disappeared in

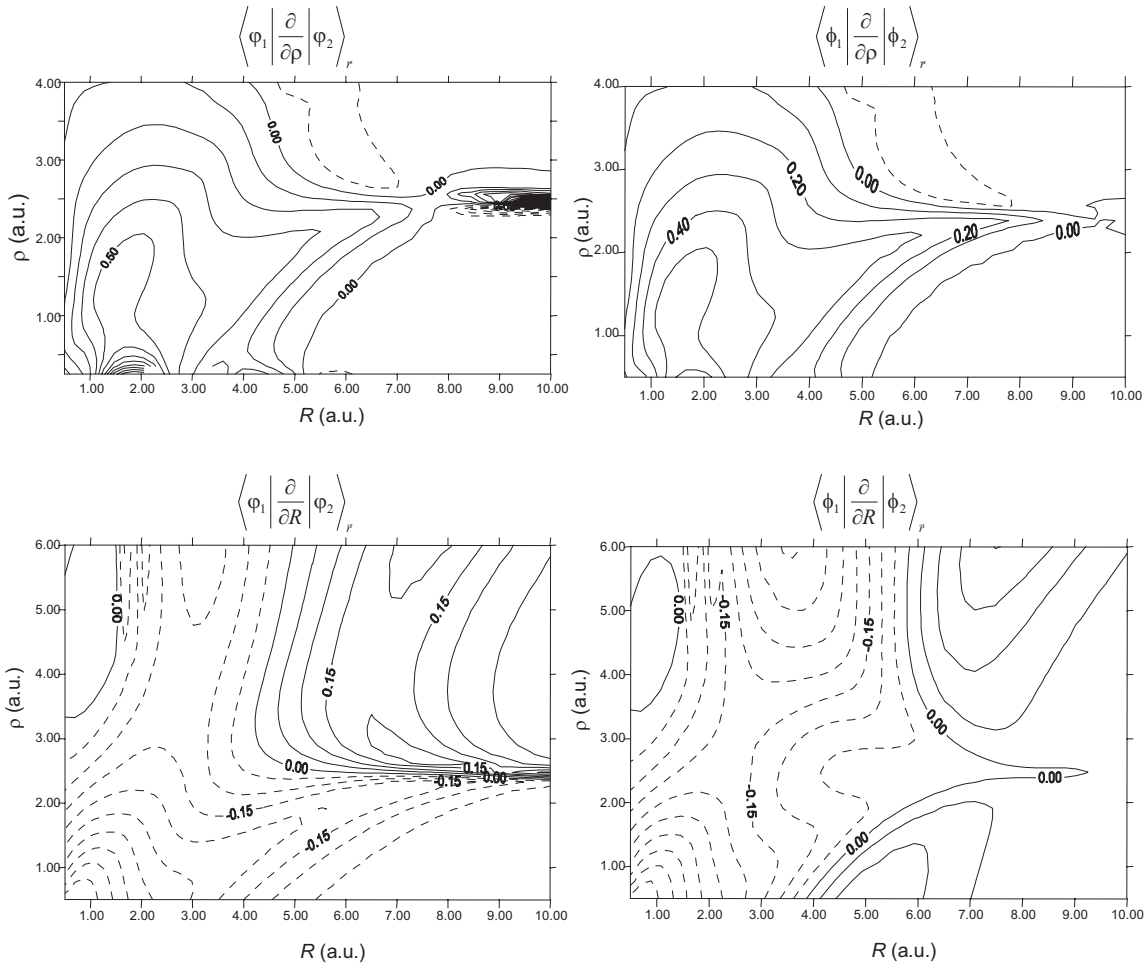

FIG. 2. Contour plots of the vibrational (top panels) and radial couplings (bottom panels) between the two lowest states of H_3^+ for $\theta=60°$. Left panels are the couplings between the adiabatic states and right panels between the diabatic states defined through Eqs. (27) and (31).

the diabatic representation. It must be noted that the transformation does not introduce any new singularity, since the new coupling H_{12} is a smooth function of the nuclear coordinates.

IV. RESULTS

A. Total cross sections for $H^+ + H_2$ collisions

We have carried out VCC calculations within semiclassical and quantal formalisms, as explained in Sec. II. The basis set for both calculations included the two lowest electronic states of H_3^+, which dissociate as $R \to \infty$ into $H^+ + H_2(X\,^1\Sigma_g^+)$ and $H(1s) + H_2^+(X\,^2\Sigma_g^+)$, respectively, and a basis set of vibrational functions, which contained all bound and continuum states of H_2 and H_2^+ up to a dissociation energy of 0.4 a.u. In a first calculation, we have applied an isotropic approximation, where the systems of differential equations (10) and (20) are solved with the dynamical couplings evaluated for a fixed value of the angle θ (60° in our calculation). This approximation was checked for this system in the work of Ref. [39], although that work used DIM molecular wave functions and a restricted vibronic basis. Here, we have performed some additional tests that will be presented later on.

We present in Fig. 3 the calculated total cross sections for electron capture into H_2^+ bound and dissociative levels, which correspond to the sum of cross sections for processes (3) and (4). We also include in this figure the cross sections for total excitation [H_2 vibrational excitation (1) and dissociation (2)]. Our cross sections are compared with experimental data for electron capture of [8,10,40] and previous calculations for electronic capture of [11,14] and for vibrational excitation of [11]. The recommended data of Phelps [6], as explained by the author, are a compromise between several experiments; they approach the data of Ref. [8] at $E>60$ eV and follow a smooth curve that approaches those of Ref. [41], not shown in Fig. 3, at $E<5$ eV. The data of Phelps for vibrational excitation were taken from the classical calculation of Ref. [42], which considered the three first excited levels of H_2. We also show in this figure the comparison with new results using the SEIKON method, which are practically identical to previous values of Ref. [20]. Also recent calculations of Kusakabe *et al.* [9,10] yielded cross sections almost indistinguishable from those of Ref. [20], and they are not shown in the figure for clarity. For comparison purposes, we have plotted in the same figure the total

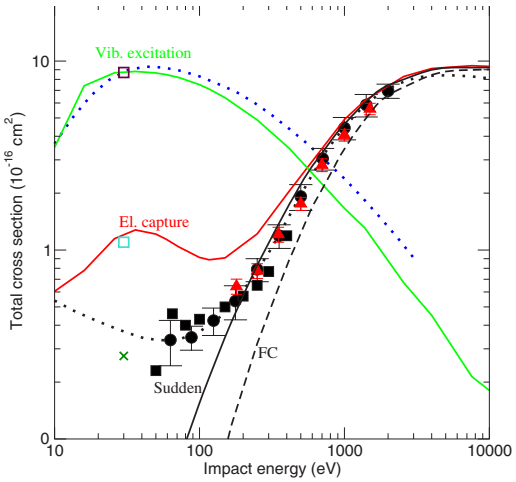

FIG. 3. (Color online) Total cross sections for vibrational excitation and electron capture processes. Solid line: present VCC eikonal calculation. Calculations using additional approximations for electron capture: solid line labeled Sudden, SEIKON approximation; dashed line labeled FC, FC approximation. Previous theoretical results: □ [11] and × [14]. Experimental results: ● [8], ▲ [10], and ■ [40]. Dotted lines: recommended data of Ref. [6].

cross section for electron capture evaluated using the FC approximation.

One can note in Fig. 3 that the VCC results for vibrational excitation agree with previous ones in practically the whole energy range of this figure and, for electron capture, with the SEIKON values at $E>300$ eV. In previous works [21], it was explained that the SEIKON approximation is not appropriate for $E<200$ eV, where it underestimates the capture cross section. However, the VCC results overestimate the cross section when compared with the available experimental data. On the other hand, our results agree with the values of [11] at $E=30$ eV, but not with those of [14]. To further analyze our results at low energies, we have performed some additional calculations, removing some approximations involved in the calculation presented in Fig. 3—in particular, the semiclassical and the isotropic approximations—and we have checked the convergence of the expansion

To check the validity of the eikonal approach, we have performed a quantal (IOSA) calculation (see Sec. II A) with the same vibronic basis set, whose results are plotted in Fig. 4(a). It is observed that quantal results tend to the semiclassical ones for impact energies above 250 eV, while below this energy the capture cross section from the quantal calculation is significantly lower than the corresponding eikonal values. We have studied this point by comparing the corresponding transition probabilities, and we have found that the difference is mainly due to trajectory effects. More specifically, at low energies, the electron-capture cross section is artificially increased in the straight-line calculation by transitions taking place at short internuclear distances, $b<R<R_0$, where R_0 is the classical distance of closest approach when one takes into account the trajectory deviation induced by short-range interactions. On the other hand, in the IOSA method, the Coriolis couplings are neglected. To estimate the effect of this approximation on the cross section, we have carried out semiclassical calculations for $E<200$ eV, removing these couplings, and we have checked that the results do not change. Therefore the quantal results are more accurate for $E<200$ eV. Since the vibrational excitation reaction takes place mainly at $b>2.0$ a.u., our quantal and semiclassical cross sections for this reaction agree over the whole energy range of Fig. 4(a).

To check the isotropic approximation, employed in the calculations of Figs. 3 and 4(a), we have calculated the electron-capture cross sections for several values of the angle θ, illustrated in Fig. 4(b). Although the collision is almost isotropic at high energies ($E>200$ eV), where the SEIKON approximation is adequate, at lower energies the dependence on θ is very important, as was already pointed out in Ref. [39]. However, as also found in that work, the average over θ leads to a cross section close to the isotropic result for $\theta=60°$ at $E>30$ eV. The average procedure is, however, required at $E<30$ eV. Accordingly, the orientation-averaged capture cross section of Fig. 4(b), where the quantal treatment has been applied for $E<300$ eV and the eikonal treatment for higher energies, is our best result for this reaction.

With respect to the convergence of the vibrational basis set, we have determined the values of the parameters $k_{\max}$

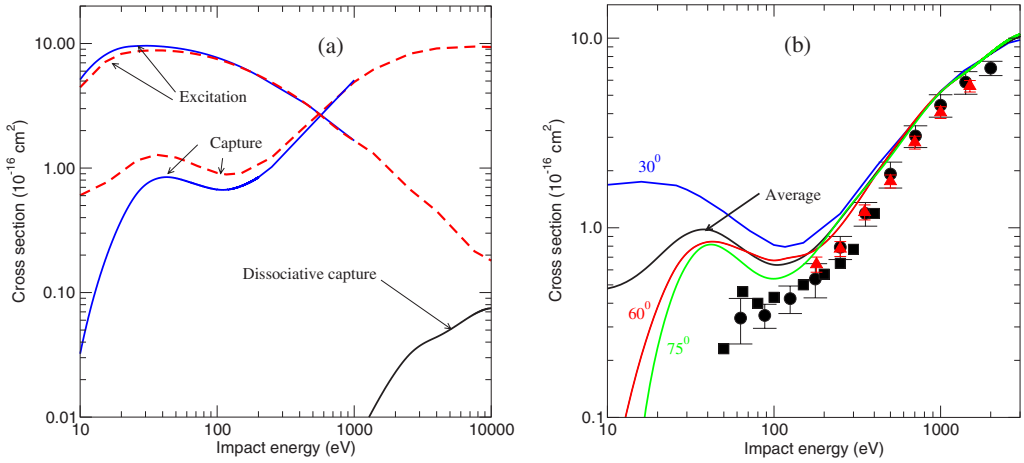

FIG. 4. (Color online) (a) Total cross sections for vibrational excitation and electron capture processes. Solid lines: quantal calculation. Dashed line: eikonal approximation. (b) Electron-capture total cross section for several values of angle θ and angular average.

and ρ_{max} by considering the convergence of the dissociation spectra, which will be explained in the next subsection. Besides, since Θ [Eq. (27)] is a function of R and ρ, the convergence of the vibronic set can be modified by the unitary transformation (27), so that we have performed two checks on the convergence of the regularized basis set. First we have employed a modified transformation angle Θ' of the form

$$\Theta' = \frac{R^2}{R^2 + \eta^2}\Theta, \tag{33}$$

with Θ given by Eq. (31) and $\eta \approx 5$ a.u. The introduction of the switching function recovers the adiabatic basis at short R. A second test is the use of the vibronic basis $\{\phi_1\chi_{1\nu}, \phi_2\chi_{1\nu}\}$ obtained multiplying both electronic wave functions by the vibrational functions defined by the H_2 potential. In this way, any unitary transformation of the electronic functions is also a unitary transformation of the vibronic basis. Although a cumbersome projection procedure is required to evaluate partial cross sections with this basis, the total capture cross section is easily obtained. Both alternative expansions lead to results identical to those presented in Fig. 4(b), and therefore, we conclude that the differences with the experiment and the maximum at $E \approx 35$ eV are not due to a distortion of the vibronic basis by the regularization procedure.

B. Partial cross sections and dissociation spectra

The cross sections for dissociative capture are shown in Fig. 4(a). For high energy, the ratio between dissociative and total electron-capture cross sections tend to the FC limit (≈ 0.01), as obtained from the corresponding FC factors. For excitation, the orthogonality of the vibrational functions leads to zero cross sections for both dissociative and nondissociative excitations in the FC limit. At low energies ($E < 100$ eV), we obtain a sizable increase of the cross sections for both dissociative reactions in the eikonal calculation, while the quantal calculation yields values smaller than 10^{-18} cm^2. We have checked that the increase found in the eikonal calculation comes from unphysical transitions in trajectories with $b < 1.0$, and accordingly these results are not shown in Fig. 4(a).

We plot in Fig. 5 the partial cross sections for population of individual vibrational states of H_2^+ and H_2 in reactions (1) and (3), respectively. The distribution over H_2^+ vibrational states after electron capture approaches the FC one as the energy increases, but for $E \leqslant 250$ eV, the ground vibrational state of H_2^+ ($\nu'=0$) is the most populated channel. It can be noted that the SEIKON method qualitatively reproduces this behavior although there are sizable differences with the VCC calculation at low energies. The process of vibrational excitation populates low-lying vibrational states, which explains the good agreement with the calculation of Ref. [42] (Fig. 3) that only considered excitations up to $\nu=3$. It is also noticeable the good agreement with the SEIKON values. An additional illustration is displayed in Fig. 6, where we have plotted the energy dependence of the excitation partial cross sections.

As already pointed out in [21], the H_2^+ vibrational distribution after electron capture at low energy can be explained

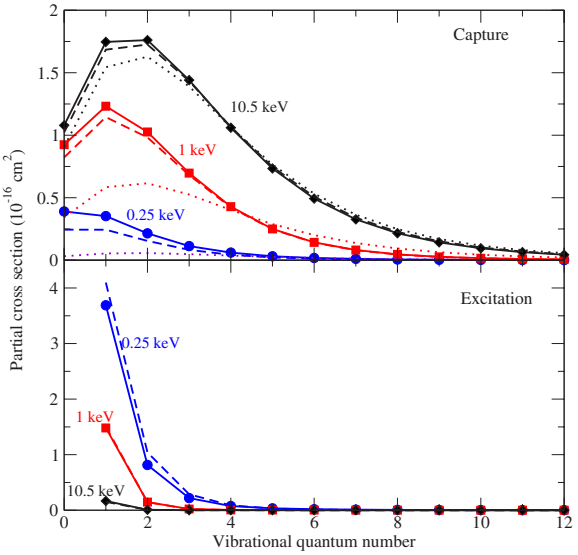

FIG. 5. (Color online) Partial cross sections. Solid lines: VCC. Dashed lines: sudden approximation. Dotted lines: Franck-Condon approximation.

by means of the quasiresonant mechanism of [15]. To illustrate this mechanism, we have diagonalized the Hamiltonian matrix in the vibronic basis, which leads to a set of adiabatic vibronic states, whose energies are displayed in Fig. 7 and where it can be noted that there is a pseudocrossing at $R \simeq 7$ a.u. between the energies of the adiabatic vibronic states that correlate to $H(1s)+H_2^+$ ($\nu=0$) and $H^+ + H_2$ ($\nu=4$). There are also series of avoided crossings at $4 < R < 7$ a.u. between the energies of capture and excitation channels where transitions are important at low energies. As already explained in previous works, at low energies, the electron-capture process takes place in two steps: first, the excitation states are populated at $R \approx 2-3$ a.u., and then the capture channels are

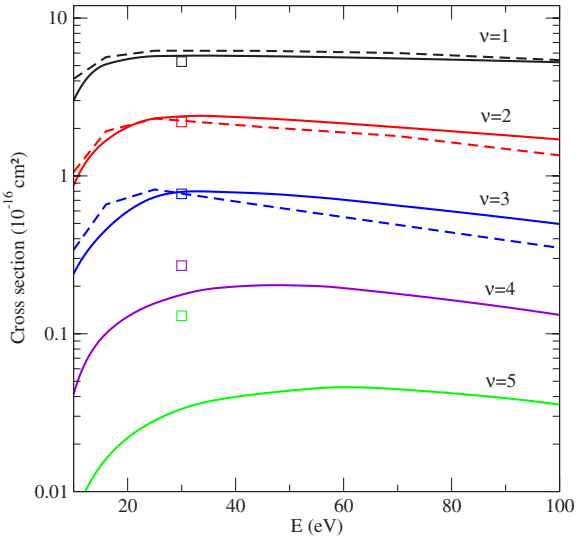

FIG. 6. (Color online) Cross sections for excitation to the H_2 vibrational states with $\nu=1-5$. Solid line: present calculation. Dashed line: classical calculation of Ref. [42]. Squares: IOSA calculation of Ref. [11].

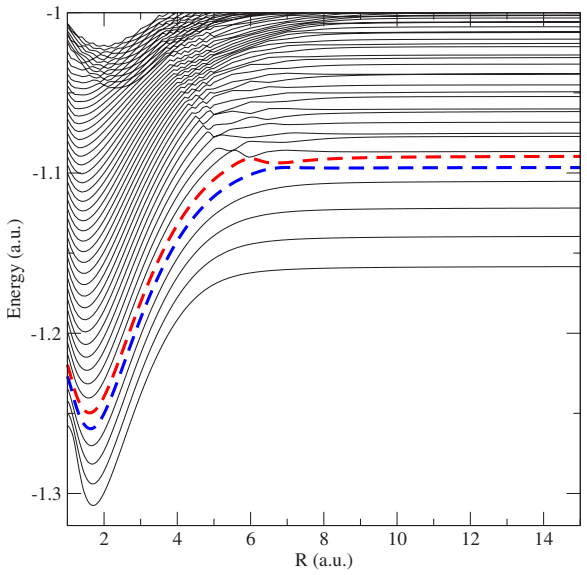

FIG. 7. (Color online) Energy curves of the 50 lowest-lying vibronic states of the H_3^+ quasimolecule for $\theta=60°$. The dashed lines are the energies of the states that correlate to $H(1s)+H_2^+(\nu=0)$ and $H^++H_2(\nu=4)$ in the limit $R\to\infty$.

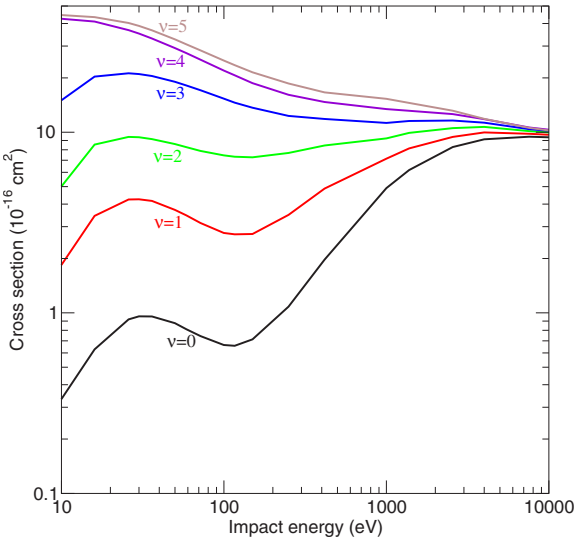

FIG. 8. (Color online) Total cross section for electron capture from several vibrational states of H_2.

populated in the way out of the collision by transitions from the excitation channels at $R\approx 5-7$ a.u., which correspond to the above-mentioned region of avoided crossings. As a consequence, the dominant exit channel of the capture reaction is the ground vibrational state of H_2^+. On the other hand, the cross sections for excitation to $\nu=3,4$ of Fig. 6 exhibit maxima at $E\approx 35$ eV, similar to the position of the local maximum in the capture cross sections; this is consistent with our explanation of the latter maximum as a consequence of the two-step mechanism. At $E>200$ eV the vibrational excitation reaction takes place as a secondary process from the capture states, as found in [21], and vibrational excitation becomes less relevant as the energy increases. According to this sudden mechanism, the populations of the H_2^+ vibrational states after reaction (3) follow the FC distribution at high impact energies (see Fig. 5).

Because of its interest in fusion research, we have also evaluated (see Fig. 8) total capture cross sections for collisions with H_2 in excited vibrational states. As in previous calculations of Refs. [12,16], we find a significant increase of the cross sections as ν increases. Besides, it is noticeable that the maximum of the cross section at $E\simeq 35$ eV does not appear in the results for collisions with excited molecules ($\nu\geqslant 4$), where the electron-capture reaction involves direct transitions from the excited entrance channels to the ground vibrational state of H_2^+.

The VCC with a discretized representation of the vibrational continua allows us to obtain the dissociation spectra; the spectrum is defined as $d\sigma(E_d)/dE_d$, with $\sigma(E_d)$ the cross section for transition to a dissociative state of energy E_d. As an illustration, we plot in Fig. 9 these spectra for reactions (2) and (4) at three representative impact energies. As a check of the convergence of the expansion, we show in this figure our impact-parameter-VCC results for three sets of values of the parameters $\rho_{\max}$ and $k_{\max}$. We also compare the VCC results with those obtained with the SEIKON method. As for the case of partial cross sections for bound states, we obtain a reasonable agreement between both calculations for capture, although some oscillations are noticeable in the VCC calculation at $E=0.25$ keV. We have not included in the second panel of Fig. 9 our results for $E>1$ keV, because they are very small.

To further analyze the spectra at low impact energies, we have plotted in Fig. 10 the comparison of the VCC spectrum for dissociative capture from $H_2(\nu=0)$ with the results of

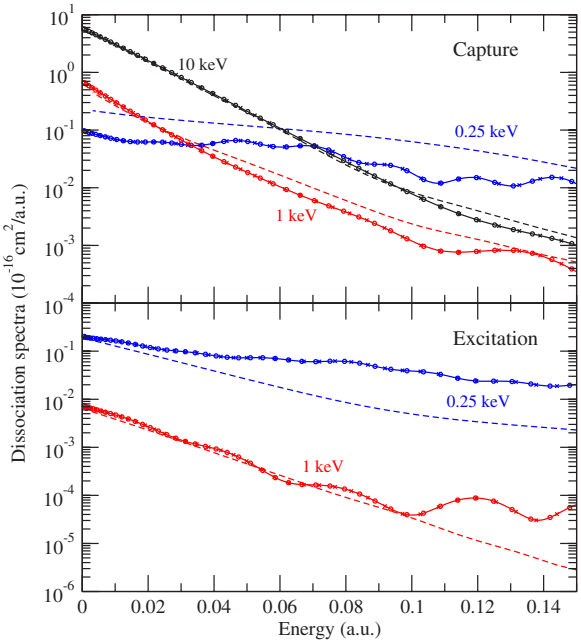

FIG. 9. (Color online) Dissociation spectra for three impact energies as indicated in the figure. Solid lines: VCC with $\rho_{\max}=10$ a.u., $k_{\max}=40$ a.u. (●) VCC with $\rho_{\max}=20$ a.u., $k_{\max}=40$ a.u. (×) VCC with $\rho_{\max}=10$ a.u., $\rho_{\max}=30$ a.u. Dashed line: SEIKON approximation.

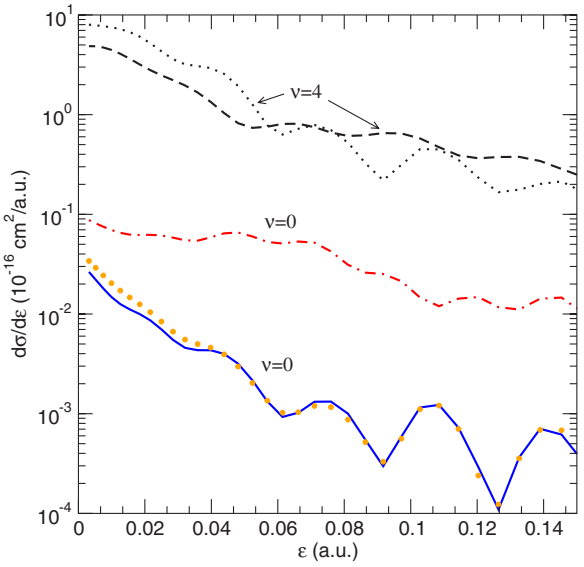

FIG. 10. (Color online) Spectra for dissociative capture in $H^+ + H_2(\nu)$ collisions at $E=250$ eV. Dotted line: SEIKON result for $\nu=4$. Dashed line: semiclassical VCC result for $\nu=4$. Dot-dashed line: semiclassical VCC result for $\nu=0$. Solid line: quantal VCC result for $\nu=0$. (●) Semiclassical VCC result for $\nu=0$ including only trajectories with $b>1$ a.u.

applying the sudden and VCC approximations for collisions with vibrationally excited molecules $[H_2(\nu=4)]$, which exhibit similar oscillations. The comparison shown in this figure, together with additional tests on the shape of the vibrational functions and transition amplitudes points out to the following explanation of the oscillations.

(i) In the SEIKON approach, the amplitude for transition from the vibrational state χ_ν to a discretized continuum state χ_ε is given by (see [18])

$$a_{\nu\varepsilon}(b,v) = \int d\rho\, \chi_\nu a(\rho,b,v)\chi_\varepsilon, \tag{34}$$

where the coefficients $a(\rho,b,v)$ are obtained in a dynamical calculation for fixed internuclear distance ρ. Since χ_0 is localized in a narrow region of values of ρ, where $a(\rho,b,v)$ is practically constant, the integral with $\nu=0$ in Eq. (32) is proportional to $\int d\rho\, \chi_0\chi_\varepsilon$, the square root of the Franck-Condon factor, which is a smooth function of ε, explaining the nonoscillatory shape of the SEIKON result for the corresponding spectra.

(ii) Using similar arguments, the SEIKON results for $a_{4,\varepsilon}(b,v)$ are oscillatory functions of ε because of the larger extension of the wave function $\chi_4(\rho)$. As a consequence, the oscillations in the VCC spectrum for collisions with $\chi_0(\rho)$ can be interpreted as due to a two-step mechanism of the dissociative capture process, similar to that explained previously for the nondissociative reaction, where the first step involves the excitation to $\nu=3,4$ vibrational levels.

(iii) Although the mechanism is correctly described by the eikonal treatment, the cross section is increased by nonphysical transitions at low impact parameters. This is also shown in Fig. 10, where we have included the quantal results and the semiclassical ones, where trajectories with $b<1.0$ a.u. have not been included in the calculation of the dissociative capture cross section.

C. Isotope effect

In Fig. 11 we present total electron-capture cross sections for H^+ collisions with different isotopical variants of the target molecule, compared with the recent experimental data of [10]. Since these experiments have been performed at $E>100$ eV, we have restricted the energy range in this figure. In our calculations, the molecules are initially in the ground vibrational state and the cross sections have been evaluated by applying the quantal treatment for $E<250$ eV and the semiclassical one for higher impact energies. The isotope effect (see [10]) is qualitatively interpreted by taking into account that the increase of the reduced mass involves a larger number of vibrational states below the exit channel $H_2(\nu'=0)$, and therefore a higher excitation is required to produce the capture process. Additionally, for the heavy species, the vibrational initial state is more localized near the equilibrium distance, and thus the FC approximation, which yields a small capture cross section, becomes more appropriate as the reduced mass increases. This is further illustrated in the last panel of Fig. 11, where we compare the capture cross sections for several isotopic variants.

V. CONCLUSIONS

We have reported close-coupling calculations of electron-capture and vibrational excitation processes in $H^+ + H_2$ collisions, including total and state-to-state cross sections and dissociation spectra. We have also evaluated total cross sections for isotopically modified target molecules and for H_2 in excited vibrational states. To cover the impact energy range 0.01–10 keV, we have applied the VCC treatment with a discretized representation of the vibrational continuum.

The first aim of our calculation was to confirm the cross sections reported in previous calculations. In general, our results for electron capture agree with previous ones, based on the sudden approximation for molecular vibration, for $E>300$ eV. The agreement is less satisfactory for vibrational excitation.

As already pointed out by Kusakabe *et al.* [10], the region of energies below 200 eV is particularly difficult; in this energy region, the capture cross section is one order of magnitude smaller than the cross section for vibrational excitation, and while the calculation of the cross section for the dominant process is relatively easy, the capture cross sections is more sensitive to changes in the basis employed. Accordingly, we have employed *ab initio* PES's for the electronic states of H_3^+, which have been carefully regularized to remove the singular couplings due to the asymptotic conical seam, and we have employed a large vibrational basis set in terms of spherical Bessel functions. The convergence of our results with respect to the size of the basis and the regularization procedure has been explicitly studied. Besides, at energies below 200 eV, trajectory effects become sizable, and we have applied a full quantal formalism. We thus believe

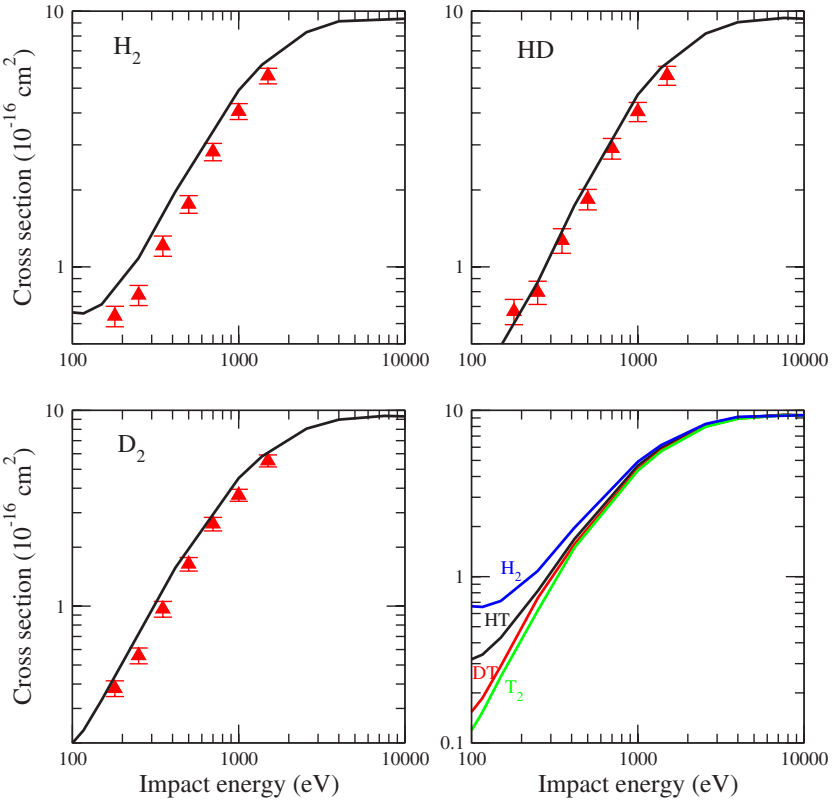

FIG. 11. (Color online) Total cross sections for electron capture in collisions of H^+ with different isotopical variants of the hydrogen molecule, as indicated in the figure. The experimental cross sections have been reported in Ref. [10].

that our results are the most accurate obtained in the framework of the IOSA method. An unexpected result is the maximum of the capture cross section at $E \simeq 35$ eV, where our cross section agrees with the calculation of Baer *et al.* [11]. We have explained the origin of this maximum as a consequence of the quasiresonant mechanism, which involves transitions between the vibronic states dissociating into $H^+ + H_2$ $(v=4)$ and $H(1s)+H_2^+$ $(v'=0)$. This local maximum in the capture cross section does not appear in the recommended data of Ref. [6]; nevertheless, it must be recalled that these data are obtained by interpolating the existing experimental values between 5 and 60 eV, and new measurements at low energy are required. From the theoretical side, the use of methods beyond the sudden approximation for rotation and probably the inclusion of the hydrogen exchange process are needed to extend the calculations to lower energies.

With respect to the vibrational excitation reaction, we obtain general good agreement with the classical calculation of Ref. [42], but some discrepancies are found at low energies $(E<30$ eV) where quantal effects are expected to be significant. The discretization of H_2 and H_2^+ vibrational continua has allowed the computation of cross sections and spectra for the dissociative reactions (2) and (4), which are in general small compared to the total cross sections for excitation and electron capture. The spectra exhibit oscillatory behaviors with respect the fragment energy in the low-impact-energy range. These behaviors stem from a two-step mechanism of the dissociation process similar to that found for the nondissociative capture reaction.

ACKNOWLEDGMENT

This work has been partially supported by DGICYT Projects No. ENE2004-06266 and No. FIS2004-04145.

[1] R. K. Janev, At. Plasma-Mater. Interact. Data Fusion **9**, 1 (2001).
[2] T. E. Cravens, Science **296**, 1042 (2002).
[3] M. B. Shah and H. B. Gilbody, J. Phys. B **15**, 3441 (1982).
[4] M. B. Shah, P. McCallion, and H. B. Gilbody, J. Phys. B **24**, 3983 (1989).
[5] C. Illescas and A. Riera, J. Phys. B **31**, 2777 (1998).
[6] A. V. Phelps, J. Phys. Chem. Ref. Data **19**, 653 (1990).
[7] T. Tabata and T. Shirai, At. Data Nucl. Data Tables **76**, 1 (2000).
[8] M. W. Gealy and B. Van Zyl, Phys. Rev. A **36**, 3091 (1987).
[9] T. Kusakabe, M. Kimura, L. Pichl, R. J. Buenker, and H. Tawara, Phys. Rev. A **68**, 050701(R) (2003).
[10] T. Kusakabe, L. Pichl, R. J. Buenker, M. Kimura, and H. Tawara, Phys. Rev. A **70**, 052710 (2004).
[11] M. Baer, G. Niedner-Schatteburg, and J. P. Toennies, J. Chem. Phys. **91**, 4169 (1989).
[12] P. S. Krstić, Phys. Rev. A **66**, 042717 (2002).
[13] P. S. Krstić and R. K. Janev, Phys. Rev. A **67**, 022708 (2003).
[14] J. Morales, A. Diz, E. Deumens, and Y. Öhrn, J. Chem. Phys.

103, 9968 (1995).
[15] G. Niedner, M. Noll, J. P. Toennies, and C. Schlier, J. Chem. Phys. **87**, 2685 (1987).
[16] A. Ichihara, O. Iwamoto, and R. Janev, J. Phys. B **33**, 4747 (2000).
[17] R. K. Preston and J. C. Tully, J. Chem. Phys. **54**, 4297 (1971).
[18] L. F. Errea, J. D. Gorfinkiel, A. Macías, L. Méndez, and A. Riera, J. Phys. B **30**, 3855 (1997).
[19] M. Kimura, Phys. Rev. A **32**, 802 (1985).
[20] D. Elizaga, L. F. Errea, J. D. Gorfinkiel, A. Macías, L. Méndez, A. Riera, and A. Rojas, J. Phys. B **33**, 2037 (2000).
[21] L. F. Errea, A. Macías, L. Méndez, I. Rabadán, and A. Riera, Phys. Rev. A **65**, 010701(R) (2001).
[22] L. F. Errea, J. D. Gorfinkiel, A. Macías, L. Méndez, and A. Riera, J. Phys. B **32**, 1705 (1999).
[23] P. Barragán, L. F. Errea, L. Méndez, I. Rabadán, and A. Riera, Astrophys. J. **636**, 544 (2006).
[24] F. O. Ellison, J. Am. Chem. Soc. **85**, 3540 (1963).
[25] V. Sidis, Adv. At., Mol., Opt. Phys. **26**, 161 (1990).
[26] W. R. Thorson and J. B. Delos, Phys. Rev. A **18**, 135 (1978).
[27] L. F. Errea, L. Méndez, and A. Riera, J. Phys. B **15**, 101 (1982).
[28] L. F. Errea, C. Harel, H. Jouin, L. Méndez, B. Pons, and A. Riera, J. Phys. B **31**, 3527 (1998).
[29] A. Macías and A. Riera, Phys. Rep. **81**, 299 (1982).
[30] B. R. Johnson, J. Comput. Phys. **13**, 445 (1973).
[31] S. B. Schneiderman and A. Russek, Phys. Rev. **181**, 311 (1969).
[32] E. R. Davidson, in *MOTECC, Modern Techniques in Computational Chemistry*, edited by E. Clementi (ESCOM, Leiden, 1990).
[33] B. Pons, Phys. Rev. Lett. **84**, 4569 (2000).
[34] B. Pons, Phys. Rev. A **63**, 012704 (2001).
[35] B. Pons, Phys. Rev. A **64**, 019904(E) (2001).
[36] L. F. Errea, C. Harel, H. Jouin, L. Méndez, B. Pons, A. Riera, and I. Sevila, Phys. Rev. A **65**, 022711 (2002).
[37] P. Barragán, L. F. Errea, L. Méndez, A. Macías, I. Rabadán, A. Riera, J. Lucas, and A. Aguilar, J. Chem. Phys. **121**, 11629 (2004).
[38] P. Barragán, L. F. Errea, A. Macías, L. Méndez, I. Rabadán, and A. Riera, J. Chem. Phys. **124**, 184303 (2006).
[39] L. F. Errea, A. Macías, L. Méndez, I. Rabadán, and A. Riera, Int. J. Mol. Sci. **3**, 142 (2002).
[40] W. H. Cramer, J. Chem. Phys. **35**, 836 (1961).
[41] M. G. Holliday, J. T. Muckerma, and L. Friedman, J. Chem. Phys. **54**, 1058 (1971).
[42] W. R. Gentry and C. F. Giese, Phys. Rev. A **11**, 90 (1975).